Biological applications of spectral self-interference.

Lev Moiseev [*a], Charles R. Cantor [a], Anna K. Swan [b], Bennett B Goldberg [c], and M. Selim Ünlü [b],

[a] Center for Advanced Biotechnology, Boston University, 36 Cummington St., Boston, MA 02215, USA;
[b] Department of Electrical and Computer Engineering, Boston University, 8 St. Mary's Street, Boston, MA 02215, USA;
[c] Department of Physics, Boston University, 590 Commonwealth Avenue, Boston, MA 02215, USA;

ABSTRACT

An original technique, Spectral Self-Interference Fluorescence Microscopy (SSFM), can determine the location of fluorescent markers above a reflecting surface with sub-nanometer precision. SSFM was used to resolve the position of a fluorescent marker bound to either the top or the bottom leaflet of a lipid bilayer – the difference in distance is only 4 nm. SSFM is a valuable tool in studying the conformation of DNA molecules immobilized on surfaces. A fluorescent label attached to a DNA molecule tethered to the surface can help elucidate its spatial orientation. This method is based on the fact that spontaneous emission of fluorophores located near a mirror is modified by the interference between direct and reflected waves, which leads to an oscillatory pattern in the emission spectrum. Spectral patterns of emission near surfaces can be precisely described with a classical model that considers the relative intensity and polarization state of direct and reflected waves depending on dipole orientation. An algorithm based on the emission model and polynomial fitting built into a software application can be used for fast and efficient analysis of self-interference spectra yielding information about the location of the emitters with very high precision.

Keywords: Fluorescence microscopy, interference, DNA arrays, lipid films.

1. INTRODUCTION

Interfererometry-based approaches, especially those based on self-interference, comprise a unique subclass of high-resolution fluorescence microscopy techniques[1,2]. A novel technique, spectral self-interference fluorescence microscopy (SSFM), employs interference-based modulation of the emission spectra to determine the precise location of a fluorophore above a mirror. If the separation between the emitter and the reflecting surface is large, on the order of ten λ, only a small change in the wavelength is needed to go from constructive to destructive interference. The effect of the long path difference is included in the wavelength-dependent reflection coefficient R defined for the system. The result is oscillations, or fringes, in the emission spectrum – a unique spectral signature of the height of the emitter above the reflector (Fig. 1). Small height differences produce shifts in the fringes and changes in the period of oscillation, although the latter are less apparent. The broader the emission spectrum, the more information is collected and the more precise the height determination. The distance above the mirror can be determined solely from the oscillations within the spectrum [3]. The axial position of the fluorophores is encoded in the spectral oscillations and not in the overall intensity; therefore, variations in fluorophore density, emission intensity, and the excitation field strength will not affect the apparent axial position.

[*] LEVA1M@BU.EDU

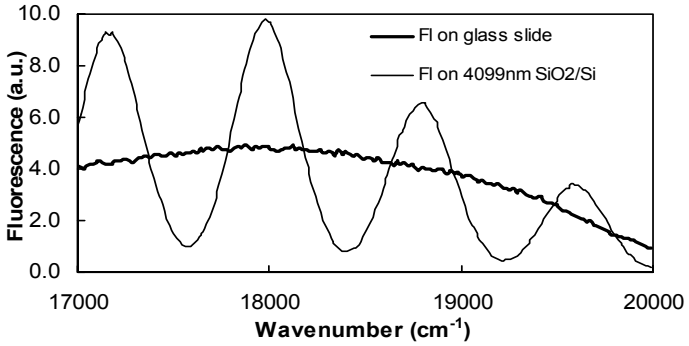

Fig. 1. Emission spectra of fluorescein monolayer on a glass slide and on a Si-SiO_2 chip with ~4μm spacer layer of oxide.

2. MATERIALS AND METHODS

All oligonucleotides used in this study were purchased lyophilized from idtdna.com and dissolved in water. The oligonucleotide concentrations were determined from absorbance measurements at 260 nm.

2.1 Preparation of Si-SiO_2 wafers

All silicon oxide chips used in the experimental part were cut from the same batch of wafers with a diamond-tipped scriber. The wafers were polished silicon with ~5 μm thick oxide layer grown by plasma-enhanced chemical vapor deposition (PECVD) [23]. Following PECVD, the wafers were chemo-mechanically polished to a measured RMS roughness to~ 2 nm.

2.2 Silanation of SiO_2 surfaces

A SiO_2-covered chip was washed with an organic solvent (acetone or ethanol) and sonicated in water for 30 min. The chip was then treated with piranha solution (H_2SO_4+30%H_2O_2 2:1 v/v) for 15-20 min. In most cases the surface of the chip became highly hydrophilic, indicating that the contaminants were removed. In some cases, an additional 15-min treatment with a mildly etching solution (NH_4OH+30%H_2O_2+H_2O 1:1:5 v/v) was necessary. This etchant was shown to dissolve about 3-5 nm of silicon oxide from the surface during the treatment time of 15 min, which did not significantly increase the roughness of the surface.

The cleaned chip, while still wet, was placed in a 5% (v/v) solution of aminopropyltriethoxysilane (APTES) in acetone containing 2% (v/v) triethylamine base (TEA) for 2 min. After silanation, the chip was washed 10 times with acetone for 5 min each time and dried at 110ºC for 20 min.

2.3 Immobilization of single- and double-stranded DNA on surfaces

Silicon oxide chips were silanized with aminopropyltriethoxysilane (APTES) as described above. A solution of the linker was prepared by dissolving 4-5 mg 1,4-phenylene diisothiocyanate (Ph-DITC) in anhydrous DMSO. The chips and the linker solution were placed in a glass vial and flushed with dry Ar. The vial was placed on a shaker at medium speed for 1 hr. The chips were then washed three times with anhydrous DMSO and one time with acetone.

10 μl of 100μM oligonucleotide labeled with a NH_2-reactive group was added to 90 μl 1M K_2HPO_4 (pH 8). The DNA solution was placed on top of the crosslinker-modified chip for 2hrs. The chip was washed 3 times with 1M NaCl Tris (pH 7) 1hr each time and stored in same buffer. If the second DNA strand was to be annealed, the chip was instead briefly rinsed with 1M NaCl Tris (pH 7), and a 10μM solution of the second strand in same buffer was placed on top of the chip and left overnight at room temperature. After annealing, the chip was washed three times in 1M NaCl Tris (pH 7) 1 hr each time.

2.4 Fabrication of Langmuir-Blodgett (LB) films on solid support

Lipid bilayers were fabricated by vertical deposition of dipalmitoyl phosphatidylethanolamine (DPPE) (1mg/ml solution in chloroform) from an air/water interface in a Langmuir-Blodgett trough at surface pressure

45 mM/m. The labeled leaflet of the lipid bilayer (either top or bottom) contained fluorescein dihexadecanoyl phosphatidylethanolamine (f-DHPE) added to DPPE at 2:100 molar ratio prior to deposition.

2.5 Microscope setup and spectral measurements

The measurements were performed on a combined microscope-spectrometer system. The microscope was an upright Leica DM/LM. A motorized microscope stage with sub-micrometer precision was used to position and scan the sample. The spectrometer was Renishaw 1000B micro-Raman system. An 1800 groove per millimeter grating was used with a spectral resolution of 2 cm^{-1} at 500 nm. The dispersed light was imaged onto a thermoelectrically cooled charge-coupled device (CCD) detector. The grating was used in a scanning mode to extend the measured wavelength range (typically 3000 cm^{-1}). A slit at the entrance of the spectrometer was closed to, typically, 30 μm.

For white light measurements the light source was a normal Koehler illumination halogen bulb. The aperture diaphragm was closed to its minimum setting in order to limit the maximum angle of incidence to ~1.4 degrees. For fluorescence measurements the light source used was an argon ion laser with a 488nm line. The laser beam was expanded to almost fill the back aperture. The laser was coupled into the microscope via a 488nm notch filter, where only the laser line is reflected. The emission from the fluorophores was collected with a 5x (NA=0.12) or 10x (NA=0.22) objective and was transmitted through the notch filter, cutting off the excitation light, into the spectrometer (Figure 2.1).

3. SELF-INTERFERENCE MODEL

In order to describe the emission pattern of a dipole near a surface, it is necessary to consider the intensity and polarization of both the direct and the reflected waves. The following model calculates the contribution of each wave that set up interference picture.

An emitting dipole with polar tilt angle θ is placed at a distance d from a stack of mirrors (Fig. 2). A detector attached to a microscope above the dipole collects a cone of light defined by the numerical aperture of the microscope objective.

Every emission direction within the collected cone can be described by θ_{em}, the tilt angle from the surface normal, and φ, the azimuthal angle to the dipole. The dipole radiates two coherent waves: one sent directly to the detector, and one incident on the mirror surface, which is then reflected so that it propagates parallel to the direct wave, Assuming the distance between the dipole and the mirror is significantly smaller than the distance between the dipole and the microscope objective, the direct and the reflected waves arriving at the same spot on the detector propagate parallel to each other.

If the near-field radiation effects are omitted, the intensity of light radiated by a classical dipole in any direction is proportional to the $\sin\alpha$, where α is the angle between the dipole vector and the direction of propagation. The emitted light is polarized in the plane defined by these two vectors. If a dipole is parallel or perpendicular to the surface, the intensity of direct and incident light are the same, because $\alpha_{inc}=\alpha_{dir}$. This is, generally, not the case for a randomly oriented dipole, i.e., the intensity and polarization of the direct and the incident waves depend on dipole orientation.

The E_{TM} component of both the incident and direct waves lies in the plane of incidence, and the E_{TE} is perpendicular to it. After reflection, the incident wave is modified by reflection coefficients R_{TE} and R_{TM} of the stack of mirrors. Additional phase shift between the direct and the reflected waves arises from the distance the incident light travels from the source to the stack of mirrors and back ($e^{i2kd\cos\theta_{em}}$).

Light intensity collected by a microscope objective with NA corresponding to maximum collection angle $\theta_{em,max}$ is integrated over $d\theta_{em}\sin\theta_{em}$. If the measured sample contains fluorophores with various orientations of their transition dipoles, the total collected light intensity is integrated over all possible dipole orientations. Usually, fluorophores in monolayers are randomly distributed in the horizontal plane, so their emission is integrated over φ; however, the range of polar tilt angles can sometimes be restricted. In any case, the emission is integrated over all possible dipole orientations.

If the separation between the fluorescent dye layer and the mirror is large enough, several oscillations of constructive and destructive interference appear within a small span of emitted wavelengths. This results in Wiener-like

fringes of interference in the emission spectrum; the phase and the contrast of the oscillations depend on the location and orientation of dipoles above the mirror.

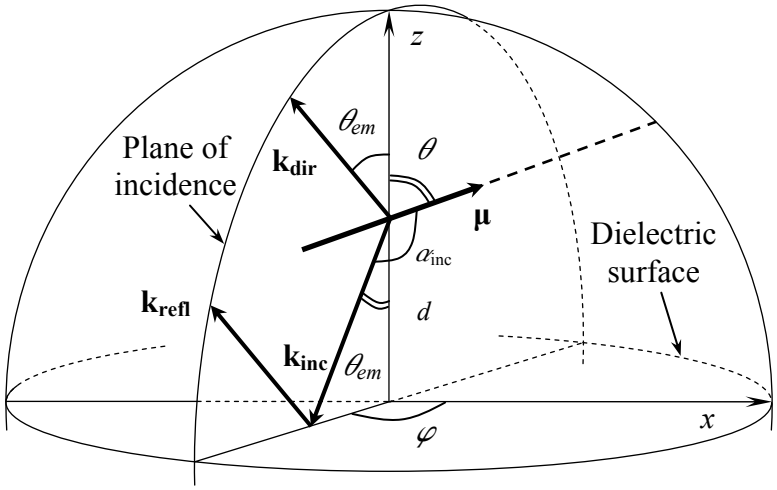

Fig. 2. Direct and reflected waves emitted by a randomly oriented dipole.

$$E_{\text{TE}dir} = E_{\text{TE}inc} \propto \cos\theta \sin\varphi$$

$$E_{\text{TM}dir/inc} \propto \sqrt{1-\left(\sin\theta_{em}\sin\theta\cos\varphi \pm \cos\theta_{em}\cos\theta\right)^2 - \sin^2\theta\sin^2\varphi}$$

$$E_{\text{TE}refl} = E_{\text{TE}inc} R_{\text{TE}} e^{i2\phi}; \qquad E_{\text{TM}refl} = E_{\text{TM}inc} R_{\text{TM}} e^{i2\phi}; \qquad \phi = \frac{4\pi n}{\lambda} d\cos\theta_{em};$$

where n is the index of refraction of the medium surrounding the dipole.

The emission of this dipole is: $I = \left|E_{\text{TE}dir} + E_{\text{TE}refl}\right|^2 + \left|E_{\text{TM}dir} + E_{\text{TM}refl}\right|^2$

The total emission of a monolayer of random dipoles measured with an objective with maximum collection angle $\theta_{em}^{\max}$:

$$I_{total} = \int_{\theta=0}^{\pi/2}\int_{\varphi=0}^{\pi/2}\int_{\theta_{em}=0}^{\theta_{em}^{\max}} I\left(\theta,\varphi,\theta_{em}\right) d\theta d\varphi d\theta_{em} \sin\theta_{em}$$

4. FITTING PROCESS

Self-interference spectra are raw data which are composed of the envelope function represented by the emission profile of the free fluorophore, the oscillatory interference component, and high-frequency Gaussian noise introduced by the spectrophotometer. The envelope function can be described by a polynomial of 5-8 degree depending on its complexity.

The interpretation of self-interference spectra can be facilitated with an algorithm that splits the spectrum into its two major components: the envelope and the oscillatory curve. Only the parameters for the oscillatory curve, such as the height of the fluorophores above the surface and the orientation of the emission transition dipoles, are used as variables in the trial-and-error fitting process. The raw spectral data is then divided by the computer-generated curve. If the parameters of the model curve accurately describe the fluorescent layer in the experiment, dividing the spectrum by the model curve will remove the oscillations produced by self-interference and leave the original spectrum that should be observed for fluorophores in the same environment, but without interference. If the parameters are off, the resulting

spectrum will still contain residual oscillations (Fig. 3). The objective is to change the parameters until dividing spectral data by the model curve leaves a smooth spectrum free from oscillations. The smoothness of the spectrum can be controlled by how well it can be fit with a polynomial function. A 5-8 degree polynomial can sufficiently closely describe a 100-150 nm span of the emission spectrum of common fluorophores. The match does not have to be perfect, as only the deviation from a smooth curve caused by self-interference oscillations is measured. The best fit is achieved when the least-squares deviation between the polynomial and the deduced spectrum of the free fluorophore goes through a minimum (Fig. 4). The algorithm can be easily incorporated into a computer program that processes an individual spectrum in seconds. When applied to experimental data, this method takes full advantage of the tremendous sensitivity of interferometry. For an emitter located on top of a silicon chip with a five-micron oxide layer, even one-nanometer deviation will cause visible distortions in the calculated free-fluorophore spectrum (Fig. 3).

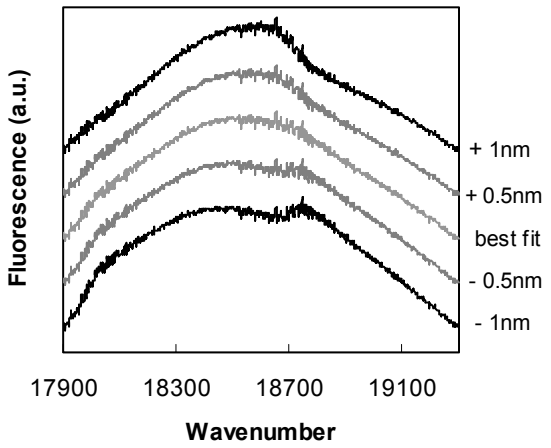

Fig. 3. Reconstructed envelope function with residual oscillations. Best fitting parameters are characterized by the smoothest envelope.

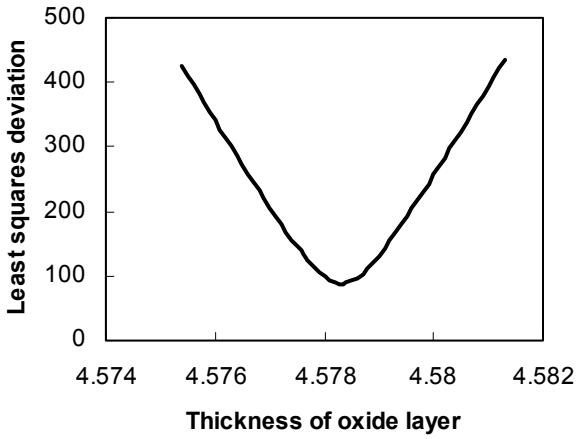

Fig. 4. Least squares deviation for the polynomial fitting of the envelope function. The minimum corresponds to the smoothest envelope.

The essence of this algorithm is that the only parameters fitted are the ones describing the oscillatory component. Since in most cases the only variable of interest is the distance between the fluorescent monolayer and the surface, fitting can be done very quickly. How is this high processing speed achieved, and how come a complex curve represented by spectral data can be fitted using only one variable? To answer this question, consider the polynomial-fitting part of the algorithm. Normally, to fit a curve consisting of an oscillatory component and a function resembling a high-degree polynomial, a large number of variables are needed to reconstruct a tentative curve and then compare it to the original data. Fitting all of 6-9 parameters for the envelope and 1-2 for the oscillatory curve at the same time is a very slow process. One can guess the overall shape of the envelope function or use emission spectra of free fluorophores in otherwise similar conditions, but this makes the fitting algorithms too complicated and also limits the reliability of the processed data. The problem is that the original spectrum of the free fluorophore may vary depending on its immediate environment, and cannot always be predicted reliably. Knowing the precise shape of the envelope function of the emission is crucial, because a slope in the envelope function will affect the position of peaks in the resulting spectral data.

The algorithm described above, however, makes an important shortcut in the fitting procedure separating the envelope function from the data in the first step. The resulting envelope function, which mimics the emission of a free fluorophore, can be independently fitted with a polynomial. The advantage of separating the fitting process of the polynomial envelope is that a function can be fitted with a polynomial (and a polynomial only) using the laws of linear algebra. Polynomial fitting is not trial-and-error fitting used for complex functions; it is done via a linear algebraic equation that calculates the parameters of the best-fitting polynom and its least-squares deviation from the original data. Taking advantage of the laws of linear algebra and the one-step polynomial fitting dramatically expedites the processing of self-interference spectral data.

5. EXPERIMENTAL RESULTS

5.1 Monolayers of fluorophores on silicon oxide surfaces - lipid films

Deposition of lipid bilayers on surfaces has attracted considerable attention because of the possibility of creating biomembrane-based biosensors and for studying the fundamental properties of biomembranes. Artificial lipid films can be used as substitutes for biomembranes in investigating the structure-function properties of various transmembrane properties in conditions similar to those found in cells. Lipid layers are an extremely versatile means with potential applications in cell biology, biocatalysis, and sensor development, but the relationship between the structure of a lipid membrane and its bioactivity must be thoroughly investigated to redeem its full value for practical use[4].

The interaction between the lipid films and various membrane-bound components can be probed by such diagnostic tools as infrared spectroscopy, neutron reflectivity, surface-plasmon resonance (SPR), and atomic force microscopy (AFM). The finest resolution of lipid surface features can be achieved by AFM, but AFM is unsuitable for probing structures that are too delicate. Also, AFM only scans the surface of the membrane and is unable to visualize buried components.

SSFM offers a unique opportunity to look inside the lipid membrane and detect the position of a fluorescently labeled component. A typical lipid bilayer has a thickness of only a few nanometers, and, of course, the position of a label cannot be determined by conventional optical methods. The following experiment was carried out in order to demonstrate the feasibility of determining the position of a fluorescent label attached to the head groups of either the top or the bottom leaflet of a lipid bilayer separated by only about 4 nm. The surface profile of a silicon-silicon oxide chip with the oxide layer thickness of about 5 μm was determined by white light interference by scanning the surface and taking reflectivity measurements at a number of locations along the scan. The optical thickness of the transparent silicon oxide layer before and after lipid deposition was obtained from the complex reflectivity of the surface over a broad wavelength range – about 100nm. A layer of DPPE containing 2% DHPE-fluorescein was deposited by the Langmuir-Blodgett technique, followed by a layer of DPPE without the dye. The fluorescence emission spectra as well as white light reflectivity measurements were taken at the same locations on the chip for which the surface profile was determined. The chip was cleaned, a new bilayer of lipids was deposited, this time the fluorescein-containing leaflet on top, and the spectra were taken again.

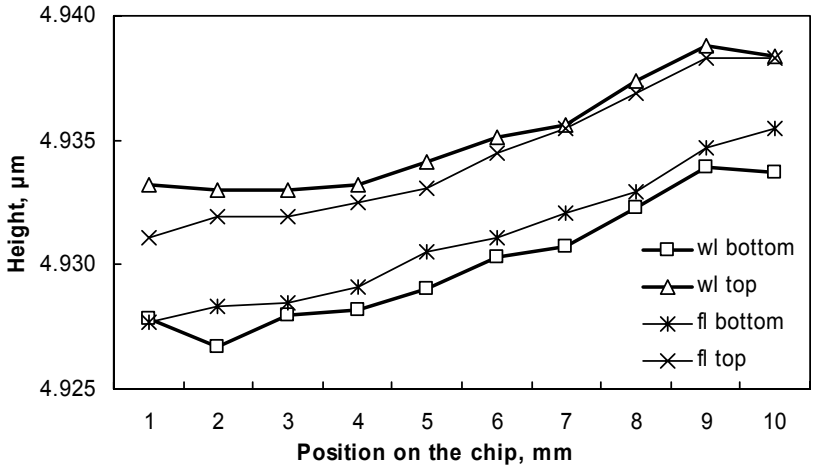

Fig. 5. Fluorescence and white light scans of lipid films.
wl bottom – white light measurement of the original surface without lipids
wl top – white light measurement of the surface with a lipid bilayer
fl bottom – SSFM measurement of a lipid bilayer with a labeled bottom layer
fl top – same, but with the labeled top layer. New bilayer was deposited for this measurement. The spectra were taken over the same precise spots on the surface of the chip in all four measurements.

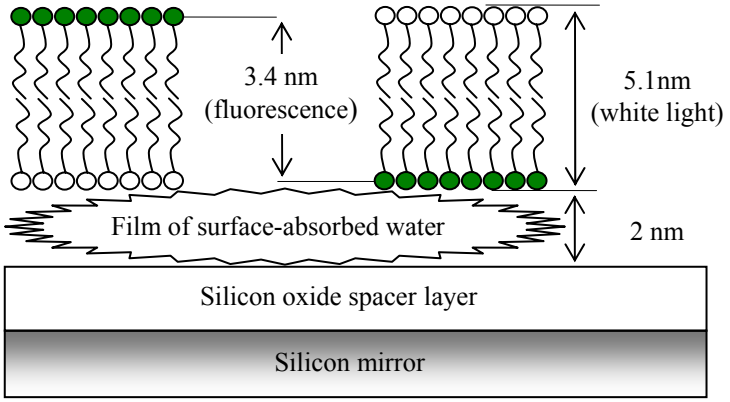

Fig. 6. Structure of the lipid bilayer based on SSFM and white light data.

The results are summarized on Figure 5. The slope of the graphs reflects the surface profile of the underlying silicon oxide layer which is rising slightly over the length of the surface scan (about 10 mm). The thickness of the bilayer film as measured by white light reflectivity was the same whether the dye-laced lipid was on top or bottom. On the other hand, the fluorescence emission spectra, as interpreted by the SSFM model, show the average position of the fluorescent dye attached to either the top or the bottom head groups, fractions of a nanometer inside the lipid bilayer (Fig. 6). Considering the surface roughness of the silicon oxide chip of about 2 nm, the accuracy of this measurement is outstanding.

5.2 Conformation of surface-immobilized DNA

One of the characteristics of a DNA array is the availability of the single-stranded probes for hybridization with the target. The conformation of DNA molecules in an array may significantly affect the efficiency of hybridization. Immobilized molecules located farther away from the solid support are closer to the solution state and are more accessible for contact with dissolved analytes. The surface, especially a hydrophobic one, acts as a shield for probes positioned close to it because of the associated steric factors and lack of diffusion of the bound molecules[5-8]. Unfortunately, little is known about the conformation of the DNA molecules immobilized on surfaces. This information can prove to be useful not only in the development and fabrication of DNA microarrays, but also in designing new applications[9].

SSFM may be a powerful tool in studying the conformation of DNA molecules immobilized on a surface. If a fluorescent label is attached to the other, free end of the DNA, the height of the label can be determined by the fluorescence interference spectra modified by the reflection in a mirror buried in the substrate (Fig. 7). The height of the label determined by the emission spectra gives the average position of the free end of the DNA molecule immobilized on the surface. Similarly, another dye of different color may be attached to a nucleotide within the DNA sequence, and the distance from the surface of another part of the oligonucleotide may be determined, even at the same time.

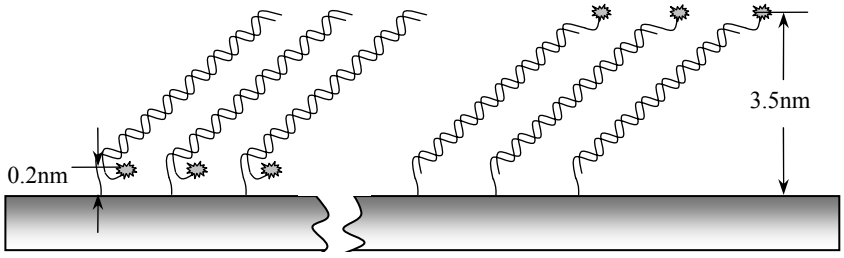

Fig. 7. Average separation between the surface and the label placed either at the proximal or distal end of a 21-bp piece of double-stranded DNA.

In this experiment an NH_2-modified oligonucleotide was tethered to the surface by its 5' end. A complementary oligonucleotide which contained a fluorescent label at either its 3'- or 5'-end was annealed to the surface-bound primer. The average height of the label above the surface was determined by SSFM and found to be ~0.2nm in the first case and ~3.5 nm in the second. The length of a 21bp piece of double stranded DNA is approximately 7nm; therefore the average tilt of the double-stranded molecules immobilized on the surface in this experiment is 33º.

SSFM carries obvious advantages over the other methods used for studying DNA conformation[10]. This method is non-contact, there are no limitations to applying it to chips submerged in a buffer, and it specifically determines the axial position of the labeled nucleotide only.

6. CONCLUSIONS

This work presents a novel method for determining the position of fluorescent markers with high precision. In practical applications, the most suitable systems for analysis with SSFM are monolayers of fluorescent markers on flat surfaces. Examples of such systems include fluorescently labeled Langmuir-Blodgett lipid films on solid substrates or DNA arrays. There are several advantages to using SSFM compared to previously describe method of studying surface-immobilized biological molecules. While SSFM cannot compare to AFM in lateral resolution, the tremendous axial precision is achieved in measuring the location of fluorescent labels inside the specimen. SSFM is a non-invasive, optical method and can be applied to such delicate substrates as surface-immobilized DNA molecules protruding into the solution.

REFERENCES

1. K. H. Drexhage, "Interaction of light with monomolecular dye layers," *Prog. Optics*. **12**, pp. 163-232, 1974.
2. A. Lambacher and P. Fromherz, "Fluorescence interference-contrast microscopy on oxidized silicon using a monomolecular dye layer," *Appl. Phys. A* **63**, 207-216, 1996.
3. A. K. Swan, L. Moiseev, C. R. Cantor, B. Davis, S. B. Ippolito, W. C. Karl, B. B. Goldberg, and M. S. Ünlü, "Towards nanometer-scale resolution in fluorescence microscopy using spectral self-interference," *IEEE JSTQE* **9** (2), pp. 294-300, 2003.
4. V. Kiessling and L. K. Tamm, "Measuring distances in supported bilayers by fluorescence interference-contrast microscopy: polymer supports and SNARE proteins," *Biophys. J.* **84**, pp. 408-418, 2003.
5. M. S. Shchepinov, S. C. Case-Green, and E. M. Southern, "Steric factors influencing hybridization of nucleic acids to oligonucleotide arrays," *Nucl. Acids Res.* **25** (6), pp. 1155-1161, 1997.
6. E. Southern, K. Mir, and M. Shchepinov, "Molecular interactions on microarrays," *Nat. Genet*. **21**, pp. 5-9, 1999.
7. K. U. Mir and E. M. Southern, "Determining the influence of structure on hybridization using oligonucleotide arrays," *Nat. Biotech*. **17**, pp. 788-792, 1999.
8. A. Vainrub and B. M. Pettitt, "Surface electrostatic effects in oligonucleotide microarrays: Control and optimization of binding thermodynamics," *Biopolymers* **68**, pp. 265-270, 2003.
9. K.Y. Wong and M. B. Pettitt, "A study of DNA tethered to a surface by an all-atom molecular dynamics simulation," *Theor. Chem. Acc.* **106**, pp. 233-235, 2001.
10. S. O. Kelley, J. K. Barton, N. M. Jackson, L. D. McPherson, A. B. Potter, E. M. Spain, M. J. Allen, and M. G. Hill, "Orienting DNA helices on gold using applied electric fields," *Langmuir* **14** (24), pp. 6781-6784, 1998.